

# Superfluidity in two-dimensions. A thermal conductivity study of $^4\text{He}$ and $^3\text{He}$ - $^4\text{He}$ mixture films

DANIELE FINOTELLO

*Department of Physics, Kent State University  
Kent OH 44242, USA*

Recibido el 13 de agosto de 1991; aceptado el 13 de septiembre de 1991

**ABSTRACT.** We review measurements of the thermal transport of  $^4\text{He}$  films and  $^3\text{He}$ - $^4\text{He}$  mixture films near the superfluid transition. These measurements were performed on helium films of thickness ranging from 12 to 156 Å and mixture films with  $^3\text{He}$  concentration up to 2%. The superfluid transition temperature for these films ranged from 1.2 to 2.2 K. We discuss universal features of the data as well as the behavior of the ratio of the vortex diffusion constant to vortex core-parameter, the sharpness of the transition and the superfluid transition temperature as a function of thickness and concentration. We also describe new experiments that will contribute to a better understanding of the observed behavior.

PACS: 64.70.-p; 64.70.Rh; 67.70.+n

## 1. INTRODUCTION

The superfluid transition of  $^4\text{He}$  when physisorbed on a two-dimensional (2D) substrate is described in terms of the vortex-antivortex unbinding theory of Kosterlitz and Thouless (KT) [1,2]. Using renormalization group techniques, Kosterlitz and Thouless solved the problem of a dilute gas of logarithmically interacting vortex-antivortex pairs. These pairs' unbinding mechanism is a cooperative effect which destroys the algebraic long-range order of the system at a nonzero superfluid density. Many of the predictions arising from the KT theory have been extensively studied and verified [3,4].

The superfluid transition is in the same universality class as, for instance, 2D melting, the superconducting transition in thin films, and some transitions in liquid crystals. It is thus of considerable theoretical and experimental interest. Indeed, there are several aspects of the superfluid transition which merit further attention. Among them, there is the question of how this transition is modified when one deals with helium films much thicker than a few monolayers (1 layer = 3.6 Å). It is expected that, as long as one is in a temperature region where the 3D correlation length is larger than the film thickness, the 2D behavior should be manifest. If the film is made thicker, this should be modified as the critical behavior should be

relegated to a progressively narrower region in temperature as the film's  $T_c$  (the 2D superfluid transition temperature) approaches the bulk  $T_\lambda$ . It is then possible to study the universality of the KT transition in  $^4\text{He}$  films as a function of thickness. This is analogous to the study of the critical behavior at the 3D superfluid transition along the lambda line on the pressure plane [5].

In the case of liquid helium, there is, in addition, the possibility to study the universal character of the superfluid transition in the presence of  $^3\text{He}$ . When  $^3\text{He}$  is added to  $^4\text{He}$ , its effect on the superfluid transition can be viewed as an example of renormalization of a phase transition [6]. Although mixture films can be regarded as the 2D analog of 3D mixtures, they are substantially richer in possibilities because of the important roles played by the liquid-solid and liquid-vapor interfaces, as well as the arrangement of the  $^3\text{He}$  atoms relative to and along these interfaces.

In this paper we review studies of the universality of the Kosterlitz-Thouless transition as a function of thickness (pure films) and  $^3\text{He}$  concentration (mixture films). Thermal conductivity measurements were chosen as the thermodynamic probe to perform these universality studies. The thickness of the helium films ranges from  $d = 11.7$  to  $156 \text{ \AA}$ , while concentrations of  $^3\text{He}$  up to 2% were studied. The superfluid transition temperature for these films ranges from 1.28 K to nearly the lambda temperature of 2.17 K.

Below, we discuss the theoretical background behind the measurements. We follow this with a discussion of the experimental details, data and data analysis. After a summary and conclusions, we discuss possibilities for future work.

## 2. THERMAL CONDUCTION IN HELIUM FILMS

The thermal conductivity of helium films has been studied in a number of experiments [4,7]. One of the interests in this particular thermodynamic response is the fact that the transport of heat in a helium film, near the superfluid transition, is a convective process. The convective mechanism involves mass transport across the opposite ends of an experimental cell. The superfluid film flows toward a hot surface where it evaporates by absorbing latent heat. A pressure gradient then drives the gas toward the opposite cold surface where it completes the cycle by recondensing liberating its latent heat. Clearly, such a convection mechanism is realizable only when the vapor pressure of the gas is sufficiently high. In practice, this means temperatures above 1.1 K and superfluid films thicker than  $10 \text{ \AA}$ .

The superfluid phase of helium films, understood in terms of the Kosterlitz-Thouless theory, consists of a background superfluid density  $\rho_{s0}$  which is stabilized and modified by the presence of pairs of vortices of opposite circulation. At the superfluid transition, and due to thermal fluctuations, vortices paired at the largest separation become separated. This process continues as one increases the temperature further until pairs at all length scales are no longer bound. It was pointed out by Ambegaokar, Halperin, Nelson and Siggia (AHNS) [8] that the convective conduction

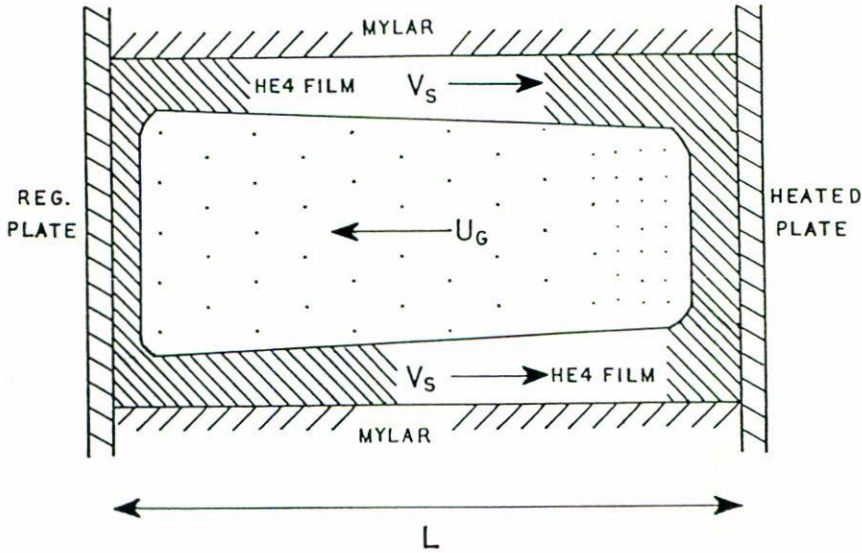


FIGURE 1. Schematics of thermal conduction experimental cell.

of a helium film near the superfluid transition should be inversely proportional to the density of free vortices  $n_f$ , hence, the square of the 2D correlation length. We note that the 2D correlation length can be viewed as the average separation of the unbound vortices. Thus, measurements of the thermal transport provide an indirect measurement of the 2D correlation length.

Expressions for the thermal conduction of helium films, appropriate for the geometry used in these experiments, were derived in great detail by Teitel [9]. The situation considered is that of an experimental chamber consisting of two parallel surfaces linking two plates (see Fig. 1). One plate is maintained at a constant temperature  $T_0$ , while the other is heated ( $Q$ ) above this by an amount  $\Delta T$ . In response to this temperature difference, the superfluid component of the helium film moves towards the heated plate. The normal (viscous) component of the film remains clamped to the substrate by its own viscosity. Helium atoms evaporate at the heated plate by absorbing latent heat. The pressure gradient, which is established across the experimental cell, drives the gas towards the cold plate where it recondenses by liberating its latent heat. In summary, the superfluid moves in one direction, while the refluxing gas moves in the opposite direction. An actual mass transport takes place.

The convective thermal transport mechanism is described by the time independent hydrodynamic equations of third sound including two modifications [9]. A dissipative term due to vortex motion must be included in the equation of the superfluid; also,  $\rho_s$ , the superfluid density which is zero above  $T_c$ , must be replaced by  $\rho_{s0}$ , the background superfluid density containing all excitations non-relevant to

the KT theory. Then, solving the modified hydrodynamic equations, one finds

$$Q = \mathcal{L} \frac{W}{L} \Delta T \left[ \left( \frac{\hbar}{m} \right)^2 \frac{D n_f}{k_B} + \frac{24\gamma T}{\rho_g^2 l^3} \right]^{-1}, \quad (1)$$

where  $\mathcal{L}$  is the latent heat,  $W$  and  $L$  are the film perimeter and the distance the film flows respectively,  $D$  is the vortex diffusion constant,  $\gamma$  the gas viscosity,  $\rho_g$  the gas density and  $l$  the spacing between parallel surfaces.

In order to extract the superfluid helium film conductivity from Eq. (1), the following considerations must be kept in mind. One must allow for the parallel heat conduction associated with the structural materials of the cell, the diffusive heat conduction of the gas itself, and, in principle, of the film as well. These contributions can be lumped together in a term  $K_b$ , a small background conductance. Also, to be able to get heat in and out of the helium film, one must overcome a boundary resistance  $K_k$ , which is in series with the convective film mechanism. Therefore, in an actual measurement, the measured thermal conductance  $K_m$  is given by

$$K_m = \frac{Q}{\Delta T} = K_b + (K_f^{-1} + K_g^{-1} + K_k^{-1})^{-1}, \quad (2)$$

where we have arbitrarily separated the film flow and gas refluxing terms as  $K_f$  and  $K_g$ . In a properly designed experiment one wants

$$K_b \ll K_f \ll K_g \approx K_k. \quad (3)$$

If Eq. (3) holds, then, from Eq. (2) we see that  $K_m \approx K_f$  yielding directly the density of free vortices. Following AHNS,  $n_f$  can be assumed to be proportional to the square of the inverse of the 2D correlation length above  $T_c$ ,

$$n_f = F \xi_+^{-2} = F a^{-2} \exp(-4\pi t^{-0.5}/b), \quad (4)$$

where  $t = (T/T_c - 1)$  is the reduced temperature, and  $b$ , is a constant which may depend on the film thickness and is not a universal number for different 2D  $XY$  systems,  $F$  is a constant of order unity reflecting the proportionality between the free vortex density and the correlation length. The constant  $a$  is the vortex core parameter which may also depend on the thickness of the helium film. From Eq. (4), we write for the film conductivity

$$\begin{aligned} K_f &= \mathcal{L}^2 F \left( \frac{W}{L} \right) \left[ k_B \left( \frac{\hbar}{m} \right)^2 \frac{D}{a^2} \right]^{-1} \exp(4\pi t^{-0.5}/b) \\ &\equiv f(T) \frac{a^2}{D} \exp(4\pi t^{-0.5}/b). \end{aligned} \quad (5)$$

From Eq. (5) we see the strong exponential temperature dependence that  $K_f$  is expected to exhibit near  $T_c$ . In an actual measurement this divergence is, however, limited by  $K_g$ ,  $K_k$  or both; and, above and away from  $T_c$ , one cannot obtain  $K_f$  once it falls substantially below the background conductivity  $K_b$ .

Measurements of the thermal conductivity of helium films are clearly very informative. In the zero power limit, they yield direct information on the values of  $D/a^2$  (up to the constant  $F$  of order unity) and  $b$ , which reflects the sharpness of the transition. These parameters, as well as  $T_c$ , can then be studied as a function of helium film thickness and the universality of the 2D superfluid transition explored. Further, if Eq. (5) holds for mixture films, the dependence of these parameters on concentration can also be studied. Finally, knowledge of the thermal conductivity of the films provides indirect information upon the behavior of the 2D correlation length.

### 3. APPARATUS AND PROCEDURE

Two experimental cells were designed to optimize our thermal conductivity studies as a function of helium film thickness. They are described below.

#### A. *Experimental cells*

The first cell used, shown at the top of Fig. 2, consisted of a strip of Mylar, 300 cm long, 2.5 cm wide and  $2.54 \mu\text{m}$  thick that was wound in a cylindrical geometry with a  $100 \mu\text{m}$  paper spacer at the ends. A relatively open space between Mylar [10] layers was ensured. This minimizes a possible viscous drag between the refluxing film and gas that could limit the convective heat transport and prevents capillary condensation. Small holes were punctured randomly in the Mylar strip to aid in vapor equilibration.

A leak-tight seal to the copper plates was achieved by using  $50 \mu\text{m}$  thick Kapton type H [10] sheet. The Kapton was formed into open end cylinders and sealed along its length with 1266 Stycast [11]. After placing the Mylar ribbon within the Kapton walls, the assembly was epoxied to the copper plates using a mixture of 1266 Stycast and copper powder. The expectation was to improve the thermal contact between the helium and the copper plates where the temperature is measured.

A heater and a germanium thermometer were positioned at the bottom plate. A second heater and a similar germanium thermometer were placed at the top plate. These previously calibrated and fairly well matched thermometers were used in a differential temperature measurement [12]. The top copper plate was also provided with a carbon glass thermometer for temperature regulation and a vapor pressure gauge [13] to monitor the pressure within the experimental cell.

The arrangement described above was found to be suitable for measuring films up to about  $58 \text{ \AA}$  thick. Thicker films were studied using the experimental cell

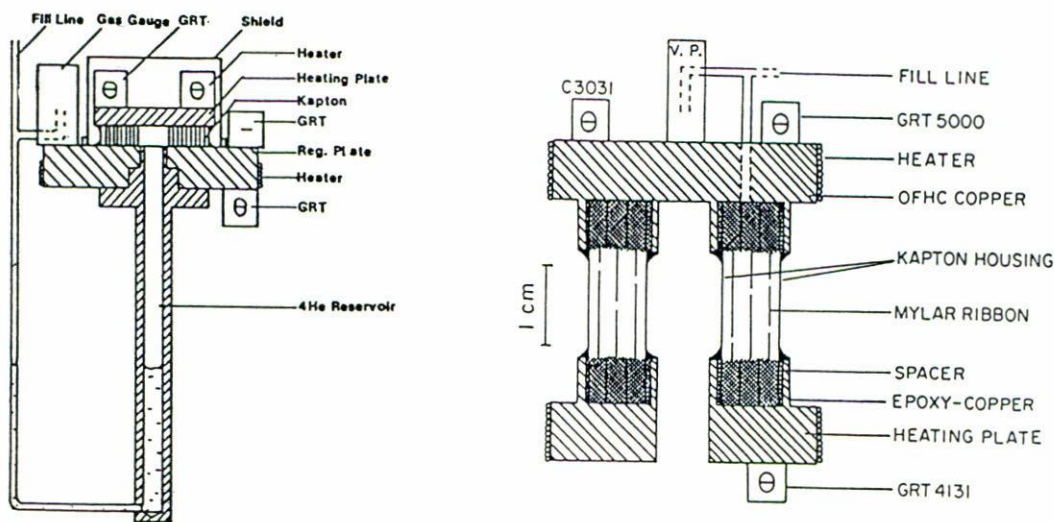


FIGURE 2. Cross sectional view of experimental cells. V.P. denotes the vapor pressure gauge. The symbol  $\theta$  denotes two germanium and one carbon glass thermometers.

shown at the bottom of Fig. 2. This consisted of two copper plates linked by 25 Kapton rings 0.44 cm wide and 50  $\mu\text{m}$  thick. The diameter of the rings increases from 1.3 to 4.2 cm in steps of about 0.1 cm. This more open arrangement avoided capillary condensation and thicker films were studied.

The thickness of the helium film in this cell is controlled by varying the liquid level in the helium reservoir attached to the bottom of the cell. The thickness as a function of height can be calculated from the van der Waals interaction of the  $^4\text{He}$  atoms with the Kapton substrate. This is done by using a procedure described in detail in Ref. [14]. In cell one, the thickness was calculated from knowledge of the low temperature surface area.

With these two cells we were able to measure films ranging in thickness from 11.7 to 156  $\text{\AA}$ , and  $T_c$  ranging from 1.28 to 2.16 K. We emphasize that possible errors in our measurements associated with film thickness are quite different in the two experimental cells. It is then very important that the results from these two cells are consistent. Measurements of mixture films were only performed using the first experimental cell.

### B. Temperature control and measurement

Temperature resolution and stability are vital in measurements of the thermal conductivity. The experimental cells were placed within light shields and attached to a  $^4\text{He}$ -evaporator which was left self-regulating at the lowest temperature ( $\approx 1.25$  K) or electronically controlled at a temperature just below that of the cell. This is

accomplished using a resistance bridge and proportional-integral-differential feedback to a heater. The cell fill line, which runs through a vacuum line to room temperature, was weakly linked to the evaporator and regulated at about 3 K.

One end of the experimental cell was regulated using the carbon glass thermometer. Better than  $1 \mu\text{K}$  regulation was achieved for most of the temperature range. The absolute temperature was determined from the germanium thermometers previously calibrated against the T58  $^4\text{He}$  vapor pressure scale [15]. The Joule-heating in the germanium thermometers was kept in the nano to pico-watts range.

To obtain the thermal conductance one has to determine the temperature difference between the regulated plate and the heated plate for a given heat input. This was accomplished via a differential temperature measurement between the two germanium thermometers. They were part of a Zair-Greenfield [16] bridge using a precision 7 decade ratio-transformer as the balancing element. Temperature differences of  $0.5 \mu\text{K}$  were reliably resolved. A more detailed discussion can be found elsewhere [12].

The procedure for data taking is as follows. A signal proportional to the temperature difference across the cell is monitored as a function of time in a strip-chart recorder. After heating the bottom plate and upon reaching equilibrium, the trace in the recorder is averaged from 5 to 30 min. for thermal noise. The conductance is determined as the ratio between the heating power applied and the temperature difference. For most of the temperature range, the conductance is determined at several heating power levels and extrapolated to the zero power limit [17]. The absolute temperature associated to each conductance data point is the average temperature of the cell. Clearly, for this average to be meaningful, the temperature difference across the cell has to be kept to a minimum.

### C. Film thickness depletion. Addition of $^3\text{He}$

As stated previously, knowledge of the low temperature surface area, which is determined from nitrogen adsorption isotherm, is necessary to calculate the helium film thickness. When helium gas is condensed from room temperature into the experimental cell, some of it remains in the gas phase in equilibrium with the film. This can be calculated from the gas pressure as measured with the *in situ* capacitive pressure gauge. Furthermore, as the temperature is increased during the measurements, some of the film is evaporated thus thinning. By monitoring the pressure changes, this film depletion can be calculated. A self-consistent correction is applied to the data so that it represents a constant film thickness conductance [12].

Finally, once the measurements with pure  $^4\text{He}$  films were completed, a  $19.1 \text{ \AA}$  film was condensed in the experimental cell. The change in pressure was monitored as small doses of  $^3\text{He}$  were added. As the addition takes place, the pressure raises quickly, eventually decreasing to an equilibrium value larger than in the pure

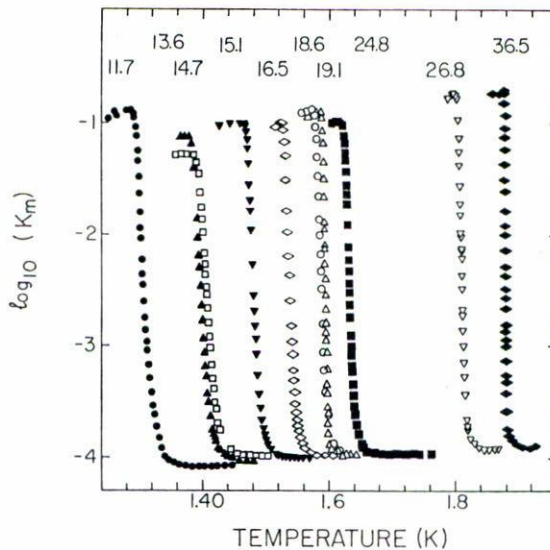


FIGURE 3. The measured conductance  $K_m$  in W/K on a log scale as a function of temperature for the ten thinnest films. Numbers refer to thickness in Å.

film case at the same temperature. Knowledge of this pressure difference allows to calculate the amount of  $^3\text{He}$  in the film. The concentration is thus defined as the amount of  $^3\text{He}$  in the film divided by the total amount of  $^3\text{He}$  and  $^4\text{He}$  in the film [18]. Proper mixing was ensured by annealing the mixture film at 4.2 K for several hours.

#### 4. DATA AND ANALYSIS

Data for our experiments have been taken over the period of several years involving the two experimental cells described above. We summarize the results in what follows.

##### A. $^4\text{He}$ films

The measured conductance  $K_m$  for all films studied is shown in Figs. 3 and 4. As already discussed, it contains contributions from several conductances (see Eq. (2)) from which the film conductance needs to be extracted. Prior to any analysis, it is evident from the above figures that, as one increases the film thickness, the superfluid transition becomes sharper. Then, the parameter  $b$  must increase with thickness.

The convective film conductance can be extracted following any of two methods described in detail in Ref. [12]. The choice of method of analysis is of no consequence

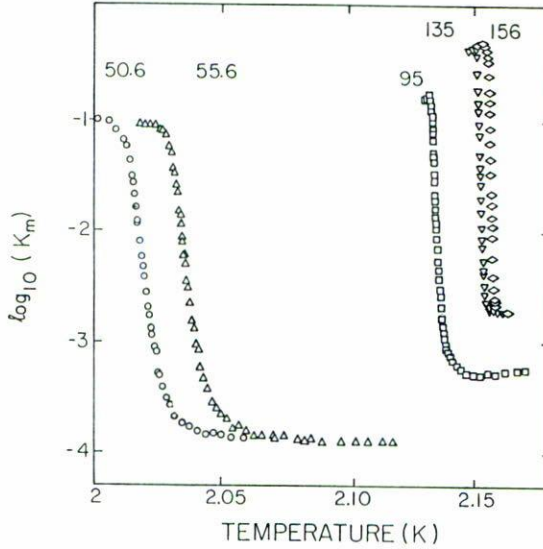


FIGURE 4. The measured conductance for thick films as a function of temperature. Notice the expanded temperature scale relative to Fig. 3.

to the general conclusions of this paper as we will emphasize trends in the data. Data analyzed using method 1 was presented in Ref. [19].

Results for some of our data as analyzed using method 2 are shown in Fig. 5. The convective film conductance changes by 4 orders of magnitude over the temperature range shown. It is evident that all films exhibit a strong singularity at the superfluid transition temperature which extends over a progressively broader region as the film becomes thinner. For the thickest film studied, this region is 3–4 mK, increasing to nearly 100 mK for an 11.7 Å thick film.

From Eq. (5) we see that the quantity  $K_f/f(T)$  can be least square fitted to extract the parameters  $D/a^2$ ,  $b$ , and  $T_c$ . This was done to obtain the solid lines shown in Fig. 6. These are semilog plots of the scaled film conductance  $K_f/f(T)$  vs  $t^{-1/2}$ . The data is expected to fall on straight lines on these plots.

The behavior of these parameters as a function of helium film thickness, or equivalently, *vs.*  $T_\lambda - T_c$ , is best illustrated in Figs. 7, 8 and 9. The most relevant features, as seen from these figures, can be summarized as follows:

1. The parameter  $D/a^2$  decreases by about three orders of magnitude as  $T_\lambda - T_c$  changes from 1 K to 0.01 K. It is about  $10^{10} \text{ sec}^{-1}$  for the thinnest films decreasing to  $10^7 \text{ sec}^{-1}$  for the thickest. This decrease might be expected both from the behavior of  $D$  and  $a$ . The diffusion constant is a measure of the ability of vortices to move along the film. This is influenced by interactions with the substrate and thermal excitations. The latter increase with temperature tending to decrease  $D$ . The vortex core parameter  $a$ , is expected to be proportional to the 3D correlation length. This

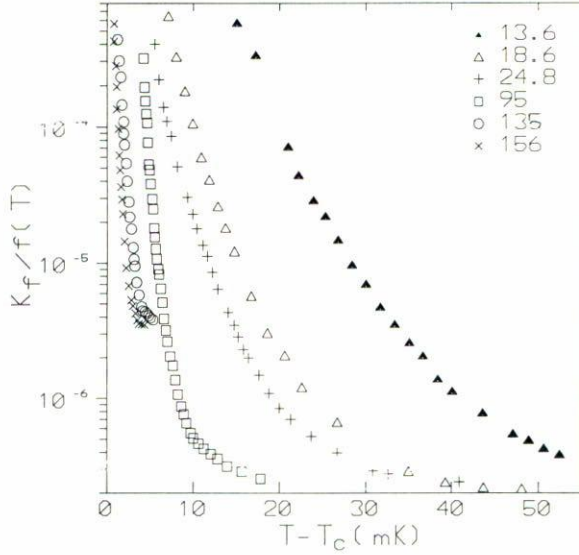


FIGURE 5. Scaled film conductance vs.  $T - T_c$  for several films.  $T_c$  for the 95 Å has been shifted by +3 mK for clarity.

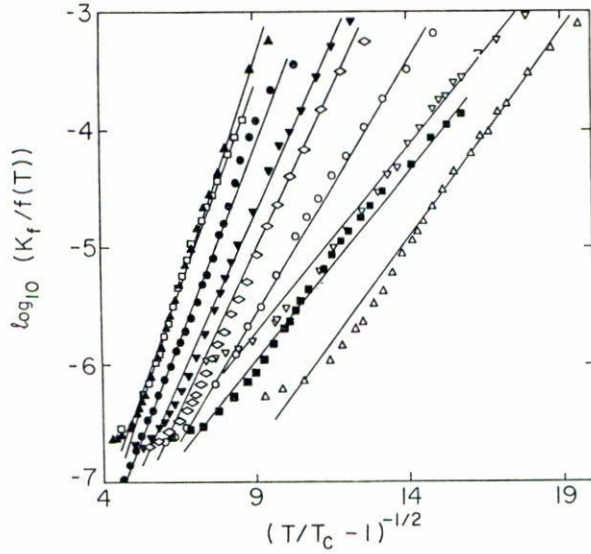


FIGURE 6. The scaled conductance plotted against  $t^{-0.5}$  to test Eq. (5). The solid lines are least squares fits. Symbols as in Fig. 3.

increases as one approaches the lambda point, eventually diverging. A larger vortex core parameter tends to decrease the ratio  $D/a^2$ .

2. The parameter  $b$ , which characterizes the sharpness of the transition, increases by approximately an order of magnitude in the same range of  $T_\lambda - T_c$ . This implies

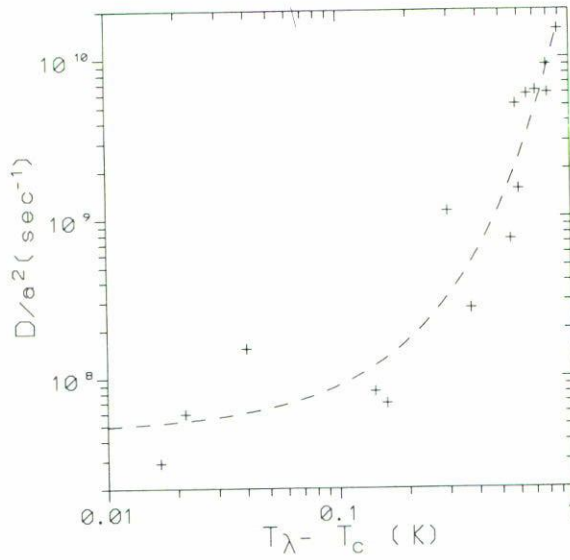


FIGURE 7. The ratio vortex diffusion constant to the square of the vortex core parameter as a function  $T_\lambda - T_c$ .

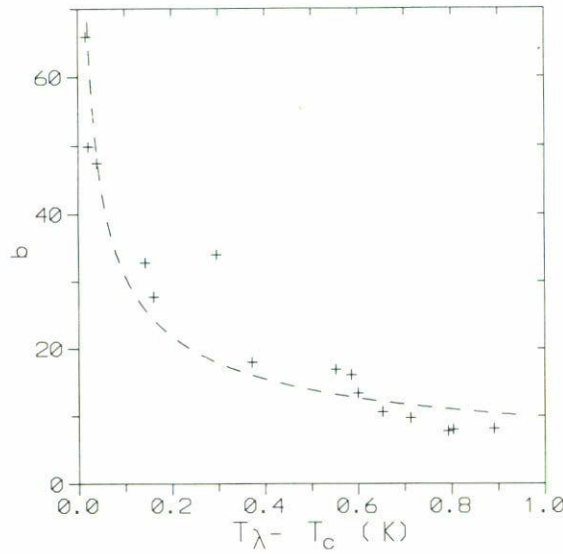


FIGURE 8. The parameter  $b$  as a function of  $T_\lambda - T_c$ .

that the 2D behavior is relegated to a narrower temperature range closer to  $T_c$  as the film thickens. In fact, the increase of  $b$  can be understood using scaling arguments involving the vortex core energy and the shift in  $T_c$  with thickness [20]. Also,  $b$  describes the strength of the  $t^{1/2}$  cusp in the superfluid density,  $\sigma_s$ , near

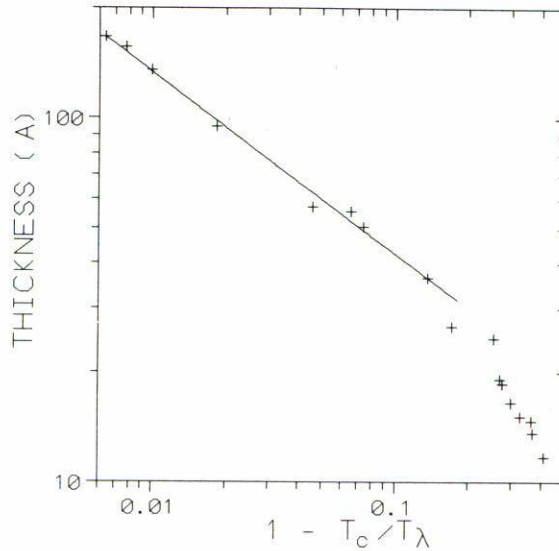


FIGURE 9. Helium film thickness against shift in critical temperature. Solid line is a least squares fit to the thick film data. See text.

$T_c$  [8]. These results imply that it becomes progressively harder for thicker films to extract the universal jump in  $\sigma_s$  at  $T_c$ .

3. The critical temperature  $T_c$ , the parameter most precisely determined from the data, as it is unaffected by the method of analysis, does not scale as expected on the basis of the 3D correlation length,  $d \propto (T_\lambda - T_c)^{-\nu}$ . One finds that for films thicker than 20 Å, an exponent of  $0.52 \pm 0.01$  instead of 0.672 is obtained. Thus, the finite size scaling hypothesis for the temperature shift does not work [14,21,22].

4. The measured conductance, even for our thickest films, shows no evidence of dimensionality crossover. For the thickest film studied, with  $T_c$  only 15 mK away from  $T_\lambda$ , the smallest value of measured conductance is several orders of magnitude above the highest measured diffusive conductance for bulk helium above  $T_\lambda$ . The data is also well described by the KT type of exponential fit. Thus, we have found no evidence of a crossover in temperature dependence from an exponential (2D) to a power law (3D).

### B. $^3\text{He}$ - $^4\text{He}$ mixture films

Once the above described measurements were completed, some of the  $^4\text{He}$  was removed from the experimental cell 1. The amount of  $^4\text{He}$  left in the cell was chosen to match the 19.1 Å film previously studied. A few data points were taken to satisfy ourselves that a good match with the original 19.1 Å film was obtained.  $^3\text{He}$  was added and several concentrations, up to 2%, studied. The cryostat was warmed up to room temperature and on a subsequent cool-down, a 14.7 Å film was

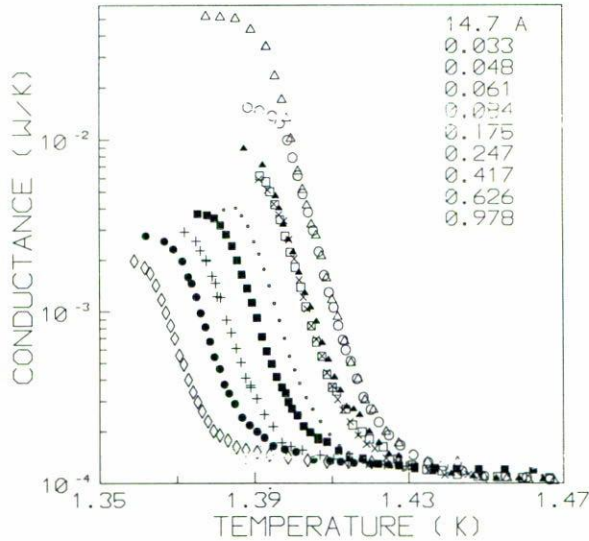


FIGURE 10. Measured conductance for a pure 14.7 Å film and several  $^3\text{He}$  concentrations. The numbers refer to the percent concentration in the film.

condensed. The thermal conductance for this pure film was measured. Doses of  $^3\text{He}$  were later added and the mixture films studied.

The measured conductance for the 14.7 and 19.1 Å films and several concentrations are shown in Figs. 10 and 11. The data are labeled by the percentage of  $^3\text{He}$  in the liquid. From these figures, several features of the data become evident as the temperature is lowered: the sharp rise associated with the superfluid transition, the shift in  $T_c$  upon addition of  $^3\text{He}$ , and the dramatic decrease in the largest measured conductance below the superfluid transition as a function of increasing concentration.

The mixture film conductance is extracted similarly to the pure films case and is shown in Fig. 12. The scaled conductance is plotted against the reduced temperature on a semilog scale to test for the critical behavior found in pure films. This is shown in Fig. 13 for both mixture films. The solid lines indicate least squares fits to the data with  $D/a^2$ ,  $b$  and  $T_c$  as parameters. The dependence on concentration of these parameters is illustrated in Fig. 14.

Based on the previous figures, the results for mixture films are summarized below:

1. The thermal response of mixture films near the superfluid transition is universal in character. The exponential divergence observed for pure films is retained for mixture films. However, a strong renormalization of the extracted parameters as a function of concentration is found.

2. The parameter  $D/a^2$  decreases sharply upon addition of  $^3\text{He}$ , reaching a nearly independent of concentration value which is a factor of 20–100 times smaller than the pure film, depending on pure film thickness. This effect might be under-

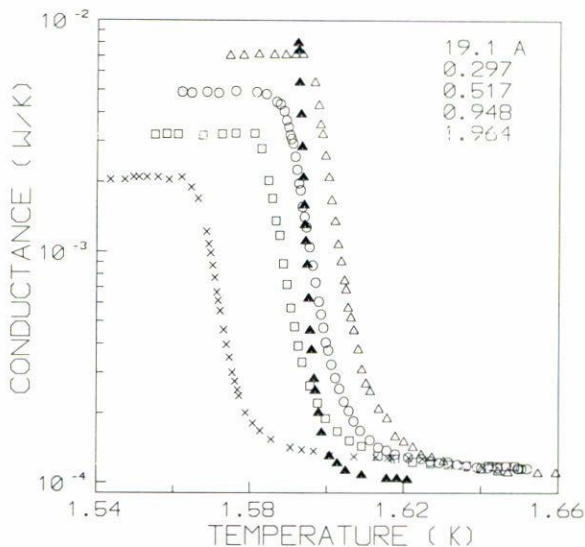


FIGURE 11. Measured conductance for a pure 19.1 Å film and several  $^3\text{He}$  concentrations. The maximum conductance (not shown) for the pure film is at 0.165 W/K. The numbers refer to the percent concentration in the film.

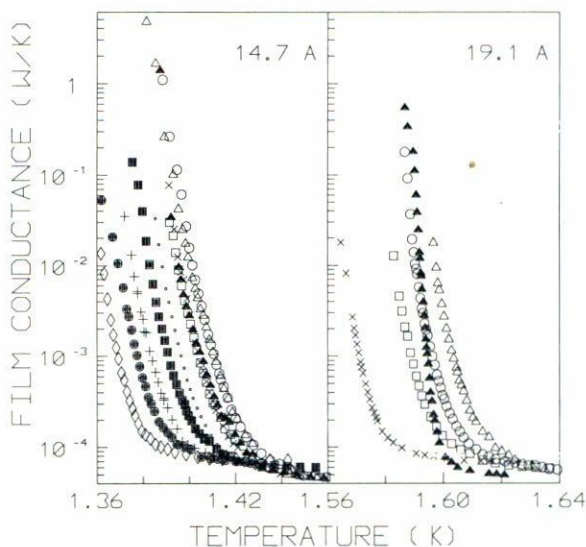


FIGURE 12. The extracted mixture films conductance. Symbols refer to concentration as in Figs. 10 and 11.

stood [18,23,24] in terms of increased scattering between the free vortices and the now present  $^3\text{He}$  normal impurity which lowers  $D$ . It can also be attributed to the added  $^3\text{He}$  atoms residing preferentially at the vortex cores. This “heavier” vortex,

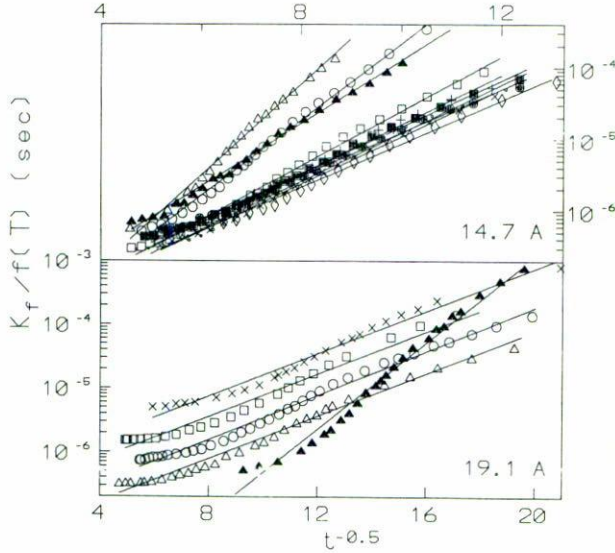


FIGURE 13. Least squares fits to the mixture films data testing for critical behavior as in pure films. Symbols refer to concentrations as in Figs. 10 and 11. The following data has been shifted up for the 19.1 Å mixture films: (o) a factor of two; (□) a factor of five; (x) a factor of ten.

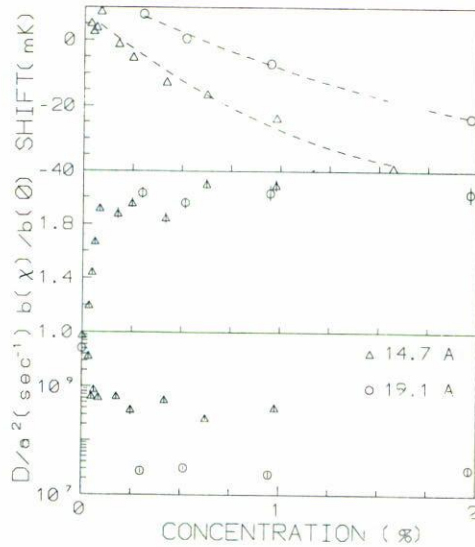


FIGURE 14.  $D/a^2$ ,  $b$  and the shift in critical temperature as a function of concentration.

of larger core radius, would find it more difficult to “diffuse”. The ratio  $D/a^2$  would be smaller as found from the measurements. The apparent threshold concentration of about 0.1% remains to be explained.

3. The parameter  $b$  increases as  $^3\text{He}$  is added, approaching a nearly independent of concentration value twice as large as that of the parent pure film. This reflects the fact that the 2D behavior take place over a narrower temperature range closer to the transition temperature. Given that  $K_f$  is proportional to  $\xi_{2D}$ , this implies that the 2D correlation length decreases upon addition of  $^3\text{He}$ . This is opposite to what is observed in bulk mixtures [25].

4. A rather striking and yet unexplained feature of the mixture data at low concentrations is the fact that the transition temperature for mixture films shifts above that of the pure film. This is contrary to the expectation of a lower transition temperature as the addition of  $^3\text{He}$  increases the normal component of the film. This trend eventually reverses at larger concentrations.

5. The largest measured conductance on the superfluid side of the transition decreases sharply upon addition of  $^3\text{He}$ . This can be partly understood in terms of a  $^3\text{He}$ - $^4\text{He}$  scattering mechanism in combination with a  $^3\text{He}$ -induced free vortex density [18,23,26].

It is evident from the above discussion that a variety of features have been unveiled via thermal conductivity. Some of the observations are rather puzzling, unexpected and yet to be explained. More work is necessary to obtain a better understanding of the observed behavior. Future experiments are detailed in the following section.

## 5. CONCLUSIONS AND FUTURE WORK

Measurements of the thermal conductivity of helium films are clearly quite informative. A great deal has been learned regarding the 2D superfluid transition. With this work we have checked the universality of this transition as a function of thickness, or, equivalently, transition temperature. We have found that the predicted exponential divergence holds for all films studied. Results from this study show a strong thickness dependence of the two characteristic parameters for the thermal conduction, namely, the ratio of diffusion constant to vortex core parameter,  $D/a^2$ , and the non-universal constant  $b$ . No crossover in dimensionality was observed as the Kosterlitz-Thouless behavior was retained up to the thickest films studied. Further, it was shown that the shift in transition temperature as a function of thickness was governed by an exponent less than that of the three-dimensional correlation length.

We have also described our measurements of the convective conductance of  $^3\text{He}$ - $^4\text{He}$  mixture films. This thermal response was tested for the critical behavior observed in pure films. This is preserved for the mixture films, *i.e.*, the exponential divergence retained. The extracted parameters  $D/a^2$  and  $b$  are, however, strongly renormalized and exhibit an unusual concentration dependence. They sharply change at low concentrations approaching a nearly concentration independent value upon exceeding a threshold concentration. The largest measured conductance was shown to drastically decrease upon addition of  $^3\text{He}$ . Also, the

transition temperature was found to increase above that of the pure film at very low concentrations.

We have pointed out several interesting and unexpected features of the data. Further experiments are therefore necessary to elucidate some of the described puzzling features of the thermal conduction data.

Regarding pure helium films, it is necessary to address the issue of dimensionality crossover. Thicker films with transition temperatures near the lambda point need to be studied. Such a study will require to improve the temperature resolution to nano-Kelvin. The non-universality of the parameter  $b$ , whose growth it is believed parallels that of the 3D correlation length, can be studied as a function of substrate. The behavior of  $D/a^2$ , changing by 3 orders of magnitude as a function of thickness, should be investigated on a different substrate. Also, helium films can be adsorbed in porous materials containing non-interconnecting nearly cylindrical pores (glass capillary arrays) or completely interconnecting pores (Vycor, Aerogel glasses). The effect of the different topologies on the superfluid behavior could then be investigated via thermal conductivity measurements. Indeed, heat capacity measurements on these porous glasses have shown to be quite interesting [27,28].

As far as  $^3\text{He}$ - $^4\text{He}$  mixture films, there are even more open questions. Mixture films thinner and thicker than measured in this work need to be studied. These studies should emphasize the low concentration regime. In fact, several orders of magnitude in concentration are experimentally accessible. Then, the dependence of  $D/a^2$  and  $b$  on concentration could be accurately established. A complete diagram  $D/a^2$  or  $b$ - $^4\text{He}$  thickness- $^3\text{He}$ - $^4\text{He}$  concentration will be generated. Functional dependencies will be established. Such studies will also allow to follow the anomalous shift in transition temperature above that of the parent pure film more accurately. One should also explore if the largest measured conductance decreases continuously with the addition of  $^3\text{He}$  or an asymptotic value is obtained. These measurements will clearly contribute to the understanding of the mechanism governing these effects.

In conclusion, thermal conductivity measurements have provided extremely interesting results that need to be pursued further. Some of the proposed experiments are presently underway at Kent State.

#### ACKNOWLEDGMENTS

I am grateful to many people for their ideas, discussions and supervision. I am deeply indebted to Frank Gasparini for his guidance and suggestions and Yao Yu who generated a great deal of data. I am also very grateful to UNAM, México for awarding a fellowship that allowed me to pursue this research at SUNY Buffalo. The experimental work at Buffalo was supported by NSF Grants DMR-8601848 and DMR-8905771. I would also like to acknowledge support from NSF Grant DMR-9013979 and The Research Council of Kent State University while this work was written.

## REFERENCES

1. J.M. Kosterlitz and D.J. Thouless, *J. Phys.* **C6** (1973) 1191; J.M. Kosterlitz, *J. Phys.* **C7** (1974) 1046.
2. D.R. Nelson and J.M. Kosterlitz, *Phys. Rev. Lett.* **39** (1977) 1201.
3. I. Rudnick, *Phys. Rev. Lett.* **40** (1978) 1454; D.J. Bishop and J.D. Reppy, *ibid.* **40** (1978) 1727.
4. J. Maps and R.B. Hallock, *Phys. Rev. Lett.* **47** (1981) 1533; G. Agnolet, S.L. Teitel and J.D. Reppy, *ibid.* **47** (1981) 1537.
5. G. Ahlers, *The Physics of Liquid and Solid Helium*, ed. K.H. Benneman and L.B. Ketterson, Wiley, New York (1975).
6. M.E. Fisher, *Phys. Rev.* **176** (1968) 257.
7. R.A. Joseph and F.M. Gasparini, *Physica* **109 & 110B + C** (1982) 2102; G.B. Hess and R.J. Muirhead, *J. Low Temp. Phys.* **49** (1982) 481.
8. V. Ambegaokar, B.I. Halperin, D.R. Nelson, and E.D. Siggia, *Phys. Rev.* **B30** (1980) 1806.
9. S.L. Teitel, *J. Low Temp. Phys.* **46** (1982) 77.
10. Mylar and Kapton are registered trademarks of the E.I. DuPont De Nemours and Co.
11. Emerson Cumming, Inc., Canton, Ma.
12. D. Finotello, Y.Y. Yu and F.M. Gasparini, *Phys. Rev.* **B41** (1990) 10994.
13. The vapor pressure gauge was designed after that of Greywall and Busch, *Rev. Sci. Instrum.* **51** (1980) 509.
14. Y.Y. Yu, D. Finotello and F.M. Gasparini, *Phys. Rev.* **B39** (1989) 6519.
15. F.G. Brickwedde, H. van Dijk, M. Duriex, J.R. Clement and J.R. Logan, *The 1958 <sup>4</sup>He Scale of Temperatures*, U.S. Government Printing Office, Washington D.C. (1960).
16. E. Zair and A.J. Greenfield, *Rev. Sci. Instrum.* **44** (1973) 695.
17. D. Finotello, Ph. D. Thesis, SUNY at Buffalo (1985).
18. Y.Y. Yu, D. Finotello and F. M. Gasparini, *J. Low. Temp. Phys.* **81** (1990) 269.
19. D. Finotello and F.M. Gasparini, *Phys. Rev. Lett.* **55** (1985) 2156.
20. R.G. Petschek, *Phys. Rev. Lett.* **57** (1986) 501.
21. D. Finotello, Y.Y. Yu, X.F. Wang and F.M. Gasparini, *Physica* **B165 & 166** (1990) 519.
22. X.F. Wang, I. Rhee and F.M. Gasparini, *Physica* **B165 & 166** (1990) 593.
23. D. Finotello, Y.Y. Yu and F.M. Gasparini, *Phys. Rev. Lett.* **57** (1986) 843.
24. R.M. Ostermeier and W.I. Glaberson, *J. Low Temp. Phys.* **20** (1975) 159.
25. G. Ahlers, as in Ref. [5] and references therein.
26. D. Finotello, Y.Y. Yu and F.M. Gasparini, *Physica* **B165 & 166** (1990) 767.
27. L.M. Steele and D. Finotello, *BAPS* **36** (1991) 870.
28. D. Finotello, K.A. Gillis, A. Wong and M.H.W. Chan, *Phys. Rev. Lett.* **61** (1988) 1954.

RESUMEN. Revisamos mediciones del transporte térmico de películas de  $^4\text{He}$  y mezclas de  $^3\text{He}$ - $^4\text{He}$  cerca de la transición superfluida. Presentamos un resumen de los resultados obtenidos con películas de helio con un espesor desde 12 a 156 Å y mezclas con concentración de  $^3\text{He}$  hasta 2%. El rango de temperatura en estas mediciones es de 1.2 a 2.2 K. Discutimos propiedades universales de estas mediciones como también el comportamiento de la constante de difusión de vórtices, el rango de temperatura y la temperatura crítica de la transición superfluida como función del espesor y de la concentración de las películas estudiadas. Describimos nuevos experimentos que contribuirán a entender el comportamiento observado